Nitric oxide-producing microglia mediate thrombin-induced degeneration of dopaminergic neurons in rat midbrain slice culture

doi: 10.1111/j.1471-4159.2006.03752.x

Nitric oxide-producing microglia mediate thrombin-induced degeneration of dopaminergic neurons in rat midbrain slice culture

Hiroshi Katsuki, Mitsugi Okawara, Haruki Shibata, Toshiaki Kume, and Akinori Akaike

Department of Pharmacology, Graduate School of Pharmaceutical Sciences, Kyoto University, Sakyo-ku, Kyoto, Japan

Address correspondence to:

Akinori Akaike, Ph.D.

Department of Pharmacology, Graduate School of Pharmaceutical Sciences,

Kyoto University

46-29 Yoshida-shimoadachi-cho, Sakyo-ku, Kyoto 606-8501, Japan

Phone: +81-75-753-4550 FAX: +81-75-753-4579

E-mail: aakaike@pharm.kyoto-u.ac.jp

Abbreviations used: ERK, extracellular signal-regulated kinase; FeTPPS, 5,10,15,20-tetrakis-(4-sulfonatophenyl)-porphyrinato-iron(III) chloride; GAD, glutamic acid decarboxylase; iNOS, inducible nitric oxide synthase; JNK, c-Jun *N*-terminal kinase; LDH, lactate dehydrogenase; MAPK, mitogen-activated protein kinase; NO, nitric oxide; PD, Parkinson's disease; PI, propidium iodide; SDS, sodium dodecyl sulfate; TH, tyrosine hydroxylase

Abstract

Activated microglia are considered to play important roles in degenerative processes of midbrain dopaminergic neurons. Here we examined mechanisms of neurotoxicity of thrombin, a protease known to trigger microglial activation, in organotypic midbrain slice cultures. Thrombin induced a progressive decline in the number of dopaminergic neurons, an increase in nitric oxide (NO) production, and whole tissue injury indicated by lactate dehydrogenase release and propidium iodide uptake. Microglia expressed inducible NO synthase (iNOS) in response to thrombin, and inhibiton of iNOS rescued dopaminergic neurons without affecting whole tissue injury. Inhibitors of mitogen-activated protein kinases (MAPKs) such as ERK, p38 MAPK and JNK attenuated thrombin-induced iNOS induction and dopaminergic cell death. Whole tissue injury was also attenuated by inhibition of ERK and p38 MAPK. Moreover, depletion of resident microglia from midbrain slices abrogated thrombin-induced NO production and dopaminergic cell death, but did not inhibit tissue injury. Finally, antioxidative drugs prevented thrombin-induced dopaminergic cell death without affecting whole tissue injury. Hence, NO production resulting from MAPK-dependent microglial iNOS induction is a crucial event in thrombin-induced dopaminergic neurodegeneration, whereas damage of other midbrain cells is MAPK-dependent but is NO-independent.

Keywords: Dopamine neuron; Inflammation; Mitogen-activated protein kinase; Neurodegeneration; Parkinson disease

Running title: Thrombin-induced dopaminergic cell death

Brain inflammatory reactions are characterized by activation of glial cells such as astrocytes and microglia. Particularly, microglia respond to various types of brain injury including trauma, ischemia and hemorrhage, and appear to act as guard cells by removing the debris of injured cells and promoting neurite regeneration (Kreutzberg 1996). On the other hand, aberrant microglial activation may be harmful to surviving neurons (Stoll an Jander 1999), because activated microglia can produce diverse sets of diffusible cytotoxic factors, namely, cytokines/chemokines, reactive oxygen species and nitric oxide (NO).

Local inflammatory reactions are observed in various neurodegenerative disorders including Alzheimer's disease and Parkinson's disease (PD). In PD, selective degeneration of dopaminergic neurons is accompanied by accumulation of a large number of reactive microglia in the substantia nigra (McGeer *et al.* 1988; Hirsch *et al.* 1998). Inflammatory reactions around degenerating dopaminergic neurons are also found in experimental models of PD such as MPTP-treated mice and monkeys (Kurkowska-Jastrzebska *et al.* 1999; McGeer *et al.* 2003). Several lines of evidence suggest that expression of inducible NO synthase (iNOS) in microglia and a resultant increase in NO production are involved in degeneration of dopaminergic neurons. In fact, iNOS expression is increased in microglia in the substantia nigra of PD patients (Knott *et al.* 2000). Mice lacking iNOS gene are resistant to MPTP toxicity (Liberatore *et al.* 1999), and pharmacological inhibition of iNOS *in vivo* rescues dopaminergic neurons from lipopolysaccharide-induced degeneration in rats (Iravani *et al.* 2002). In this context, we have demonstrated in organotypic midbrain slice cultures that NO derived from microglial iNOS plays a crucial role in degeneration of dopaminergic neurons induced by interferon-γ and lipopolysaccharide (Shibata *et al.* 2003). Peroxynitrite anion ($ONOO^-$) formed by reaction of NO with superoxide anion is generally considered to be

responsible for NO cytotoxicity, because $ONOO^-$ can produce hydroxyl radical, an extremely reactive species (Lipton *et al.* 1993).

In the present study we focused on thrombin. This serine protease, well known to play a pivotal role in blood coagulation cascade, may also act as a signaling molecule in the brain (Xie *et al.* 2003). Protease-activated receptors that mediate biological actions of thrombin are distributed widely throughout the central nervous system, and are expressed in neurons, astrocytes and microglia (Noobakhsh *et al.* 2003). One of the established actions of thrombin on brain cells is the ability to activate microglia, which is accompanied by induction of iNOS (Ryu *et al.* 2000; Suo *et al.* 2002). When injected into the substantia nigra *in vivo*, thrombin causes degeneration of dopaminergic neurons, which appears to be mediated by activation of microglia (Carreno-Muller *et al.* 2003; Choi *et al.* 2003a), and a non-selective NOS inhibitor partially inhibits thrombin-induced dopaminergic neurodegeneration *in vivo* (Choi *et al.* 2003a). On the other hand, thrombin can induce dopaminergic cell death in dissociated midbrain cultures devoid of microglia, suggesting possible direct actions of thrombin onto neurons (Choi *et al.* 2003b). Direct cytotoxic actions of thrombin have also been described in cultured hippocampal neurons (Donovan *et al.* 1997; Suo *et al.* 2003). Here, using midbrain slice cultures, we investigated whether microglial activation is a crucial step for induction of dopaminergic cell death by thrombin. Organotypic slice cultures maintain tissue architecture observed *in vivo*, thus are suitable for examinations of the mechanisms of neurodegeneration involving cell-to-cell interactions. In this study, particular attention was paid to the roles of iNOS induction, and also to the potential involvement of mitogen-activated protein kinases (MAPKs). MAPKs such as extracellular signal-regulated kinase (ERK), p38 MAPK and c-Jun *N*-terminal kinase (JNK) are known to regulate cell

survival and death under various conditions (Davis 2000; Gallo and Johnson 2002; Colucci-D'Amato *et al.* 2003). Several members of MAPK family have been reported to mediate biological responses to thrombin, including microglial activation (Ryu *et al.* 2000) and neuronal death (Choi *et al.* 2003a; Suo *et al.* 2003).

Materials and Methods

Culture preparation

Organotypic midbrain slice cultures were prepared according to the methods described previously (Shibata *et al.* 2003). All procedures were approved by our institutional animal experimentation committee, and animals were treated in accordance with the Guidelines of the United States National Institutes of Health regarding the care and use of animals for experimental procedures. Briefly, postnatal 2 - 3 day-old Wistar rats (Nihon SLC, Shizuoka, Japan) were anesthetized by hypothermia and were decapitated, the brain was removed from the skull and separated into two hemispheres. Coronal midbrain slices (350 μm thick) were prepared under sterile conditions and transferred onto microporous membranes (Millicell-CM, Millipore, Bedford, MA, U.S.A.) in 6-well plates. Six slices from one hemisphere were placed together in one membrane. Culture medium, consisting of 50% minimal essential medium/HEPES, 25% Hanks' balanced salt solution and 25% heat-inactivated horse serum (Invitrogen Japan, Tokyo, Japan) supplemented with 6.5 mg/ml glucose, 2 mM L-glutamine and 10 U/ml penicillin-G / 10 μg/ml streptomycin, was supplied at a volume of 0.76 ml per each well. The culture medium was exchanged with fresh medium on the next day of culture preparation, and thereafter, every two days. Slices were maintained in a 34°C, 5%

CO_2 humidified atmosphere.

Drug treatment

At 16 - 17 days *in vitro*, slices were exposed to thrombin (T4648, Sigma-Aldrich Chemicals, St. Louis, MO, USA) and other drugs, by transfer of culture inserts to culture plates filled with 0.76 ml of drug-containing serum-free medium. Serum-free medium consisted of 75% minimal essential medium/HEPES and 25% Hanks' balanced salt solution supplemented with 6.5 mg/ml glucose, 2 mM L-glutamine and 10 U/ml penicillin-G / 10 μg/ml streptomycin. Aminoguanidine and clodronate were purchased from Sigma-Aldrich Chemicals. 1400W, PD98059, SB203580 and 5,10,15,20-tetrakis-(4-sulfonatophenyl)-porphyrinato-iron(III) chloride (FeTPPS) were from Calbiochem (San Diego, CA, USA). SP600125 and N^{ω}-propyl-L-arginine were obtained from Tocris Cookson (Bristol, UK). *N*-acetylcysteine was from Nacalai Tesque (Kyoto, Japan).

Immunohistochemistry

After drug treatment, cultures were fixed with 4% paraformaldehyde in 0.1 M phosphate buffer containing 4% sucrose for 2 h, and whole slice cultures without sectioning were processed for tyrosine hydroxylase (TH) immunohistochemistry as described (Shibata *et al.* 2003). We used rabbit anti-TH polyclonal antibody (1:500, AB-152, Chemicon International, Temecula, CA, USA) as the primary antibody, and biotinylated anti-rabbit IgG from goat (1:200, Vector Lab., Burlingame, CA, USA) as the secondary antibody. After incubation with the secondary antibody, cultures were treated with avidin-biotinylated horseradish peroxidase complex (Vectastain Elite ABC kit, Vector Lab.), and then peroxidase was

visualized with 0.07% diaminobenzidine and 0.018% H_2O_2. Specimens were dehydrated and mounted on slide glasses. Positively stained cells bearing developed dendrites that were at least more than twice as long as cell diameter were considered as viable dopaminergic neurons. The maximal number of viable dopaminergic neurons in an area of 520×670 μm^2 in individual slices was counted. Although TH-positive neurons existed as several layers of cell population, we could count the number of these neurons in a fixed area by slightly moving the focus of the microscope on the cultures along z-axis. We also performed glutamic acid decarboxylase (GAD) immunohistochemistry to identify GABAergic neurons. Procedures for GAD immunohistochemistry were the same as those for TH immunohistochemistry, except that rabbit anti-$GAD_{65/67}$ polyclonal antibody (1:500; AB1511, Chemicon) was used as the primary antibody. The number of GAD-positive neurons in an area of 520×670 μm^2 in individual slices was counted. Additionally, total number of neurons was estimated by immunohistochemistry for a neuronal marker NeuN, with the use of mouse anti-NeuN monoclonal antibody (1:500, Chemicon) as the primary antibody and biotinylated anti-mouse IgG from horse (1:200, Vector Lab.) as the secondary antibody.

For confirmation of microglial depletion (see below), immunohistochemical examinations were performed on OX42, a marker of microglia. In this case, the primary antibody was mouse anti-OX42 (1:200, Serotec Ltd., Oxford, UK), and biotinylated anti-mouse IgG from horse (1:200, Vector Lab.) was used as the secondary antibody. Other procedures were the same as those for TH immunohistochemistry.

In several experiments, double immunofluorescence histochemistry was done for OX42 with iNOS, phospho-ERK or phospho-JNK. Primary antibodies for detection of iNOS, phospho-ERK and phospho-JNK were rabbit anti-iNOS (1:200, BD Transduction Lab., San

Diego, CA, USA), rabbit anti-phospho-p44/42 MAP kinase (T202/Y204) (1:200, Cell Signaling Technology, Beverly, MA, USA) and rabbit anti-phospho-JNK (1:200, Cell Signaling Technology), respectively. Alexa Fluor 488-labeled goat anti-mouse IgG (1:1000, Molecular Probes, Eugene, OR, USA) and Alexa Fluor 568-labeled goat anti-rabbit IgG (1:1000, Molecular Probes) were used as secondary antibodies.

Nitrite quantification

Amount of NO released during thrombin treatment was quantified as concentrations of nitrite in culture medium by Griess method. One hundred μl of culture supernatants was collected and reacted with an equal volume of Griess reagent (1% sulfanilamide and 0.1% *N*-(1-naphthyl)-ethylenediamine dihydrochloride in 2.5% phosphoric acid) for 10 min at room temperature, and absorbance of diazonium compound was measured at 540 nm. Absolute levels of nitrite were determined with reference to a standard curve obtained from defined concentrations of sodium nitrite.

Lactate dehydrogenase release assay

Amount of lactate dehydrogenase (LDH) released into culture medium after thrombin treatment was determined by a Cytotoxicity Detection LDH kit (Kyokuto Pharmaceutical Industrial Corp., Tokyo, Japan). In this assay, NAD is reduced to NADH through the conversion of lactate to pyruvate by LDH, and NADH reduces tetrazolium into formazan dyes in the presence of diaphorase. Twenty-five μl of culture supernatants was collected and incubated with 75 μl of coloring reagent in a 96-well plate at room temperature. After incubation for 1 h, the reaction was stopped by addition of 100 μl of 1 M HCl, and the

absorbance at 570 nm was determined with the use of a microplate reader. Values were normalized with the amount of LDH released from a separate group of slices (of the same sister culture) that received 300 μM MPP^+ for 72 h as 100%. This concentration of MPP^+ caused cell damage non-specifically.

Propidium iodide uptake

In addition to LDH release, propidium iodide (PI) uptake was used for assessment of overall injury of slice cultures (Fujimoto *et al.* 2004). PI (Wako Pure Chemicals, Osaka, Japan) was applied at 5 μg/ml during drug treatment, and the fluorescence in slices was observed through an inverted fluorescence microscope with a rhodamine filter set. In experiments with FeTPPS, slices were incubated for 3 h with serum-free medium containing 5 μg/ml PI after drug treatment, then PI fluorescence was observed. Fluorescence images were captured through a monochrome chilled CCD camera (C5985, Hamamatsu Photonics, Hamamatsu, Japan), and stored images were analyzed with NIH image 1.62 software. The signal intensity of each pixel was expressed as an 8-bit value, and the averaged intensity in an area of 180 × 180 μm^2 was obtained as the fluorescence value of each slice. Fluorescence values were normalized with the intensity of fluorescence in a separate group of slice cultures that received 300 μM MPP^+ for 72 h as 100%.

Western blotting

After treatment with thrombin and drugs for indicated periods, slices were collected in buffer containing 20 mM Tris-HCl (pH 7.0), 25 mM β-glycerophosphate, 2 mM EGTA, 1% Triton X-100, 1 mM phenylmethylsulfonyl fluoride, 1% aprotinin, 2 mM dithiothreitol and 1 mM

vanadate, and homogenized on ice. Lysates were centrifuged at 15000 g at 4°C for 30 min and the protein concentration in each sample was determined with a Bio-Rad Protein Assay kit. Sample buffer containing 124 mM Tris-HCl, 4% sodium dodecyl sulfate (SDS), 4% 2-mercaptoethanol, 10% glycerol and 0.02% bromophenol blue was added to each sample, and heated at 90°C for 5 min. SDS-polyacrylamide gel electrophoresis was performed on a 10% running gel with a 3% stacking gel. After gel electrophoresis, proteins were transferred onto polyvinylidene difluoride membranes. The blots were washed with Tris-buffered saline containing 0.1% Tween 20 and blocked with 5% skimmed milk for 1 h. The membrane was incubated with mouse anti-iNOS antibody (1:1000, BD Transduction Lab.), mouse anti-phospho-p44/42 MAP kinase (T202/Y204) (1:1000, Cell Signaling Technology), rabbit anti-phospho-p38 MAP kinase (Thr180/Tyr182) (1:1000, Cell Signaling Technology), rabbit anti-p38 (1:1000, Santa Cruz Biotech., Santa Cruz, CA, USA), mouse anti-phospho-JNK (1:1000, Santa Cruz Biotech.), goat anti-actin(C-11) (1:10000, Santa Cruz Biotech.) and mouse anti-glyceraldehyde phosphate dehydrogenase antibody (1:10000, Ambion, Austin, TX, USA), overnight at 4°C. After incubation with horseradish peroxidase-conjugated secondary antibodies (Vector Lab.) at room temperature for 1 h, bands were detected with enhanced chemiluminescence detection system (Amersham Biosciences, Piscataway, NJ, USA) and exposed to Fuji X-ray film. Band intensities were analyzed with NIH image.

Microglial depletion by clodronate-containing liposomes

Liposomes containing phosphate-buffered saline or clodronate were prepared according to the methods described by Van Rooijen and Sanders (1994) and were applied to slice cultures for 24 h by addition of final liposome suspension at indicated volumes in 0.76 ml of culture

medium. Liposomes containing clodronate are selectively taken up by phagocytic cells, where clodronate exerts cytotoxicity. Successful depletion of microglia by this method has been reported in cultured rat cerebellar slices (Martin-Teva *et al.* 2004). Depletion of microglia was confirmed by OX42 immunohistochemistry as described above.

Statistical analysis

Results are expressed as means ± SEM. Statistical significance was evaluated with one-way ANOVA followed by Student-Newman-Keuls' test, and probability values less than 5% were considered significant.

Results

Thrombin induces dopaminergic cell death, NO production and whole tissue injury

Application of 300 U/ml thrombin to midbrain slice cultures for 72 h induced a marked decrease in the number of viable dopaminergic neurons. Dopaminergic neurons surviving after thrombin treatment also exhibited degeneration and atrophy of dendritic processes and shrinkage of cell bodies (Fig. 1a and b). The neurotoxic effect of thrombin on dopaminergic neurons was in a concentration-dependent manner, reaching a statistically significant level at all tested concentrations of 100 - 500 U/ml (Fig. 1c). In addition, thrombin increased nitrite levels in culture medium in a concentration-dependent manner, which reflected increase in NO production (Fig. 1d). To assess whether thrombin induces whole tissue injury, we examined amount of LDH released into culture medium. Because dopaminergic neurons comprise only a small subset of midbrain cells located in a confined area within the midbrain,

levels of LDH release essentially reflect cytotoxic damage of other cells within midbrain tissues (Shibata *et al.* 2003). Indeed, we examined total number of TH-immunoreactive cells and NeuN-immunoreactive cells in midbrain slices cultured under control conditions, and the percentage of TH-positive neurons was estimated to be 2.8% of all neurons in our slice cultures. We also determined the levels of PI uptake as an alternative method to evaluate whole tissue injury. Thrombin treatment increased LDH release into medium and PI uptake into tissues in a concentration-dependent manner (Fig. 1e, f). The effect of thrombin on these parameters reached statistical significance at 300 and 500 U/ml. The number of GABAergic neurons assessed by GAD immunohistochemistry also decreased in response to thrombin at concentrations of 300 and 500 U/ml (Fig. 1g).

We next examined time course of the effects of thrombin. A significant decrease in the number of dopaminergic neurons was detected already at 24 h after application of 300 U/ml thrombin, but the decrease was progressively evident during 72 h of thrombin treatment (Fig. 2a). Increase in nitrite concentrations exhibited a similar time-dependent change, reaching statistical significance at 48 and 72 h of thrombin treatment (Fig. 2b). On the other hand, the increase in the amount of LDH released into culture medium (Fig. 2c) and the decrease in the number of GABAergic neurons (Fig. 2d) showed a delayed pattern, reaching a significant level after 72 h.

Overall, these results indicate that thrombin induces dopaminergic cell death, NO production and whole tissue injury. In the following experiments, treatment with 300 U/ml thrombin for 72 h was employed as the standard procedure to evaluate thrombin cytotoxicity.

iNOS-derived NO mediates thrombin cytotoxicity on dopaminergic neurons but not on

other midbrain cells

To examine potential involvement of iNOS in thrombin cytotoxicity, we performed double immunofluorescence staining against iNOS and OX42, a microglial marker, on midbrain slice cultures treated with 300 U/ml thrombin for 72 h. iNOS immunoreactivity overlapped with a subset of OX42-immunoreactive cells, indicating expression of iNOS in microglia (Fig. 3a).

We next examined the effect of aminoguanidine, a drug that preferentially blocks the activity of iNOS among NOS isoforms. Concurrent application of aminoguanidine (100 - 500 μM) with thrombin markedly attenuated nitrite accumulation in medium (Fig. 3c). Dopaminergic cell death induced by thrombin was also inhibited by the same concentrations of aminoguanidine (Fig. 3b). In contrast, aminoguanidine did not provide a significant protective effect against thrombin-induced whole tissue injury, as assessed by LDH release (Fig. 3d) and PI uptake (Fig. 3e). Similar results were obtained when thrombin was applied concurrently with 1400W (30 and 100 μM), another selective inhibitor of iNOS (data not shown). N^{ω}-propyl-L-arginine (30 and 100 μM), a neuronal NOS-selective inhibitor, showed no effect on thrombin-induced dopaminergic cell death, nitrite production and whole tissue injury (data not shown).

MAPKs are involved in thrombin-induced cell death and NO production

We examined consequences of inhibition of MAPKs on thrombin actions in midbrain slice cultures. PD98059 (10 - 100 μM), a drug that compromises ERK activation by inhibiting mitogen/extracellular signal-regulated kinase, prevented thrombin-induced dopaminergic cell death (Fig. 4a). Thrombin-induced nitrite accumulation was partially but significantly inhibited by PD98059 (Fig. 4b). Notably, PD98059 also markedly attenuated

thrombin-induced whole tissue injury as assessed by LDH release (Fig. 4c) and PI uptake (data not shown). SB203580 (3 - 30 μM), an inhibitor of p38 MAPK, provided similar effects to those of PD98059: this drug potently inhibited thrombin-induced dopaminergic cell death, nitrite accumulation and whole tissue injury (Fig. 4d-f). Inhibition of nitrite accumulation by 10 - 30 μM of SB203580 was almost complete (Fig. 4e), in contrast to partial inhibition by PD98059. We also found that SP600125 (10 - 100 μM), a JNK inhibitor, blocked thrombin-induced dopaminergic cell death and nitrite accumulation in a concentration-dependent manner (Fig. 4g, h). Effect of SP600125 on thrombin-induced whole tissue injury was not obvious, partly because the drug stimulated LDH release by itself (Fig. 4i). Taken together, these results suggest that all major classes of MAPKs are involved in dopaminergic cell death and NO production induced by thrombin, and that ERK and p38 are also involved in thrombin-induced death of other midbrain cells.

MAPKs are involved in thrombin-induced iNOS expression

Effective blockade of nitrite production by MAPK inhibitors suggests that these MAPKs regulate expression of iNOS induced by thrombin. We therefore examined the relationship between iNOS expression and MAPK activation by western blot analysis and immunohistochemical examinations. iNOS expression started to increase at 12 h after the onset of thrombin application, and reached a plateau level at 24 h (Fig. 5a, e). Western blot with antibodies specific for phosphorylated forms of MAPKs revealed that activation of MAPKs preceded iNOS expression (Fig. 5a, d). The phosphorylated levels of all MAPKs increased as early as 30 min after application of thrombin. Maximal increases of phospho-ERK (4.7 fold) and phospho-JNK (2.1 fold) were observed at 3 h, and then the levels

of these phopho-MAPKs gradually declined to the control level. Phospho-p38 increased 6.4 fold at 30 min after administration of thrombin, and the elevated level persisted for 72 h (Fig. 5d). Immunofluorescence staining of OX42 combined with staining of phosho-ERK or phospho-JNK showed that intense activation of ERK and JNK occurred in microglia in slices treated with thrombin for 1 h (Fig. 5b, c).

Next we tested the effects of inhibitors of MAPKs on thrombin-induced iNOS expression (Fig. 5f). SB203580 (30 μM) concomitantly applied with thrombin almost completely blocked iNOS expression assessed at 72 h after thrombin application. PD98059 (100 μM) and SP600125 (30 μM) also significantly suppressed thrombin-induced iNOS expression.

Depletion of microglia protects dopaminergic neurons from thrombin cytotoxicity

Results so far indicated that microglial activation and iNOS expression is a crucial step for induction of dopaminergic cell death by thrombin. To substantiate this proposal, we depleted microglia from slice cultures by a method developed for macrophage depletion (Van Rooijen and Sanders 1994). Immunohistochemisitry against OX42 showed that robust increase in activated microglia induced by 72-h treatment with 300 U/ml thrombin was largely attenuated by 24-h pretreatment with clodronate-containing liposomes (Fig. 6a-d). At the same time, thrombin-induced dopaminergic cell death and nitrite accumulation were also abrogated (Fig. 6e, f). Amount of thrombin-induced LDH release was not significantly affected by pretreatment with clodronate-containing liposomes (Fig. 6g). As a control, liposomes containing phosphate-buffered saline showed no effect on dopaminergic cell death, nitrite accumulation and LDH release (data not shown). These results further indicate that microglia is essential for thrombin-induced dopaminergic cell death.

Antioxidative drugs protect dopaminergic neurons but not other midbrain cells from thrombin cytotoxicity

Finally, we examined effects of drugs that inhibit oxidative stress on thrombin cytotoxicity, to delineate the mechanisms of NO-dependent dopaminergic cell death. To determine whether $ONOO^-$ is involved in thrombin-induced dopaminergic cell death, we examined the effect of an $ONOO^-$ scavenger, FeTPPS. As shown in Fig. 7a and b, FeTPPS (30 and 100 μM) significantly inhibited thrombin-induced dopaminergic cell death but had not effect on whole tissue injury as assessed by PI uptake. Nitrite concentration and LDH release could not be examined because the color of FeTPPS itself interfered the assay. We also examined the effect of an antioxidant *N*-acetylcysteine. Concurrent application of *N*-acetylcysteine (0.3 - 3 mM) protected dopaminergic neurons from thrombin cytotoxicity in a concentration-dependent manner (Fig. 7c), whereas the drug did not affect nitrite accumulation (Fig. 7d) and whole tissue injury (Fig. 7e, f). These results indicate that $ONOO^-$-related reactive oxygen species play an important role in thrombin-induced dopaminergic cell death, although they made little contribution to injury of other midbrain cells.

Discussion

Prothrombin and protease-activated receptors are widely distributed in the central nervous system, and thrombin elicits a variety of biological responses in neurons and glial cells (Noobakhsh *et al.* 2003). Thus, thrombin-mediated signaling may play important roles in

physiological and pathological processes in the brain. Microinjection of thrombin into the substantia nigra of rats causes degeneration of dopaminergic neurons, in addition to local inflammatory reactions involving microglial activation (Carreno-Muller *et al.* 2003; Choi *et al.* 2003a, 2003b). These pathological changes are reminiscent of those observed in PD, where selective degeneration of dopaminergic neurons is accompanied by inflammatory reactions (Herrera *et al.* 2005). Although relationship between thrombin dysregulation and PD pathogenesis remains to be established, elucidation of the mechanisms of thrombin neurotoxicity may provide an important clue to understand degenerative processes of dopaminergic neurons.

We demonstrated that thrombin induced cell death in midbrain slice cultures. Comparison of the changes in the number of dopaminergic neurons, the amount of LDH release and the number of GABAergic neurons suggests that thrombin cytotoxicity exhibits some selectivity on dopaminergic neurons, because lower concentrations and shorter periods of application were sufficient for thrombin to induce dopaminergic cell death than those to induce whole tissue injury or GABAergic neuron loss. In our slice cultures, percentage of dopaminergic neurons was estimated to be less than 3 % of all neurons. Thus, although degeneration of dopaminergic neurons should be accompanied by LDH release, the amount of LDH released from these neurons makes little contribution to the total amount of LDH that reflects whole tissue injury. Concerning the selectivity, an *in vivo* study by Carreno-Muller *et al.* (2003) suggested that GABAergic neurons were not affected by thrombin, which is consistent with our observations. On the other hand, Choi *et al.* (2003b) and Lee *et al.* (2005) did not find selectivity of thrombin toxicity on dopaminergic neurons over other cell populations *in vivo* and in dissociated mesencephalic culture, respectively. We do not have

obvious explanations for this discrepany, but an interesting point that should be considered is a difference in rat strains. That is, Choi *et al.* (2003b) and Lee *et al.* (2005) used Sprague-Dawley rats, whereas Carreno-Muller *et al.* (2003) and we (this study) used Wistar rats. How the strain difference could affect selectivity of thrombin cytotoxicity is totally unknown, but this situation is reminiscent of the different sensitivity of dopaminergic neurons to MPTP between mice and rats (Giovanni *et al.* 1994) and among different mouse strains (Hamre *et al.* 1999). In this study, we chose a condition of thrombin application (300 U/ml for 72 h) that caused both robust dopaminergic cell death and whole tissue injury, to examine whether different mechanisms were involved in degeneration of different cell populations.

We particularly focused on the involvement of iNOS in thrombin cytotoxicity, because this inducible enzyme seems to play an important role in dopaminergic neurodegeneration in several experimental models and in PD brain (Liberatore *et al.* 1999; Knott *et al.* 2000). Consistent with the ability of thrombin to induce expression of iNOS (Ryu *et al.* 2000; Suo *et al.* 2002; Carreno-Muller *et al.* 2003; Choi *et al.* 2003a), we found that thrombin triggered induction of iNOS in microglia within midbrain slice cultures, which was accompanied by increased NO production. Removal of microglia by pretreatment with clodronate-containing liposomes resulted in a marked decrease in nitrite levels, confirming that iNOS-expressing microglia are responsible for NO production in response to thrombin. Moreover, effects of iNOS inhibitors and microglial depletion indicate that NO derived from microglial iNOS is instrumental to thrombin-induced dopaminergic cell death. Interestingly, NO does not contribute to thrombin-induced degeneration of other midbrain cells, because abolition of NO production by iNOS inhibitors or by depletion of microglia did not prevent whole tissue injury. This is in contrast to the case with microglial activation induced by interferon-γ and

lipopolysaccharide, where inhibition of iNOS abrogated whole tissue injury in addition to dopaminergic cell death (Shibata *et al.* 2003). Nevertheless, effective protection of dopaminergic neurons by iNOS inhibition in both models of microglial activation highlights NO as a key molecule regulating dopaminergic neurodegeneration under inflammatory conditions.

Concerning MAPK family, ERK and p38 are implicated in thrombin-induced iNOS expression in cultured microglia (Ryu *et al.* 2000) and in the substantia nigra *in vivo* (Choi *et al.* 2003a). In addition, inhibition of ERK and p38 provided significant protection of nigral dopaminergic neurons against thrombin cytotoxicity *in vivo* (Choi *et al.* 2003a). A recent study on dissociated midbrain cultures demonstrated that inhibition of p38 and JNK attenuated thrombin cytotoxicity on dopaminergic neurons (Lee *et al.* 2005). In the present study, we extended these lines of evidence by showing that JNK, in addition to ERK and p38, is involved in thrombin-induced microglial iNOS expression in midbrain tissues. We also showed that all of these MAPKs mediate thrombin-induced dopaminergic neurodegeneration, at least in part through induction of iNOS expression and NO production. Notably, PD98059 and SB203580 potently inhibited whole tissue injury, indicating that MAPKs such as ERK and p38 also mediate thrombin-induced injury of cells other than dopaminergic neurons. However, MAPK-dependent iNOS expression does not participate in this process because, as mentioned above, iNOS inhibition did not suppress whole tissue injury. Although precise mechanisms of degeneration of other midbrain cells remain to be determined, thrombin has been reported to exert cytotoxicity directly on cultured hippocampal neurons and astrocytes (Donovan *et al.* 1997). Moreover, ERK activation is implicated in thrombin cytotoxicity in a hippocampal neuronal cell line (Suo *et al.* 2003). Indeed, we

observed that PD98059 potently inhibited thrombin-induced dopaminergic cell death in spite of partial blockade of NO production. These results propose that ERK in cells other than microglia, possibly dopaminergic neurons themselves, may also be involved in induction of cell death. This possibility deserves further investigations.

We further suggest that oxidative stress is involved in thrombin-induced dopaminergic cell death. This is based on the observations that both an $ONOO^-$ scavenger FeTPPS and an antioxidant *N*-acetylcysteine protected dopaminergic neurons from thrombin cytotoxicity. Hence, NO-induced dopaminergic cell death is likely to be mediated by generation of $ONOO^-$ from the reaction of NO and superoxide anion. In this study we did not address the sources of superoxide, but a recent study showed that microinjection of thrombin into the hippocampus induced upregulation of NADPH oxidase, an enzyme well known to produce superoxide (Choi *et al.* 2005). Whether NADPH oxidase is involved in thrombin-induced dopaminergic cell death is an interesting issue to be investigated. FeTPPS and *N*-acetylcysteine did not prevent whole tissue injury induced by thrombin, which supports the idea that NO-related reactive species do not participate in degeneration of other midbrain cells.

Overall, we for the first time demonstrated that thrombin recruits different mechanisms to exert cytotoxicity onto dopaminergic neurons than those onto other midbrain cells. Thrombin activates multiple members of MAPKs such as ERK, p38 MAPK and JNK. These MAPKs are involved in expression of iNOS in microglia, which causes robust increases in NO production. NO plays a critical role in degeneration of dopaminergic neurons through the conversion to $ONOO^-$. On the other hand, in spite of its dependency on MAPK activation, degeneration of other midbrain cells occurs independently of

microglia-derived NO. Different mechanisms of thrombin cytotoxicity between dopaminergic neurons and other midbrain cells may reflect the fact that dopaminergic neurons are intrinsically vulnerable to oxidative stress (Jenner 2003), which constitutes a basis of selective degeneration of these neurons in PD brain.

Acknowledgments

This study was supported by Grant-in-Aid for Scientific Research from Japan Society for the Promotion of Science and The Ministry of Education, Culture, Sports, Science and Technology, Japan. H. S. was supported by 21st Century COE Program "Knowledge Information Infrastructure for Genome Science".

References

Carreno-Muller E., Herrera A. J., de Pablos R. M., Tomas-Camardiel M., Venero J. L., Cano J. and Machado A. (2003) Thrombin induces *in vivo* degeneration of nigral dopaminergic neurons along with the activation of microglia. *J. Neurochem.* **84,** 1201-1214.

Choi S.-H., Joe E. H. Kim S. U. and Jin B. K. (2003a) Thrombin-induced microglial activation produces degeneration of nigral dopaminergic neurons *in vivo*. *J. Neurosci.* **23,** 5877-5886.

Choi S.-H., Lee D. Y., Ryu J. K., Kim J., Joe E. H. and Jin B. K. (2003b) Thrombin induces nigral dopaminergic neurodegeneration in vivo by altering expression of death-related proteins. *Neurobiol. Dis.* **14,** 181-193.

Choi S.-H., Lee D. Y., Kim S. U. and Jin B. K. (2005) Thrombin-induced oxidative stress contributes to the death of hippocampal neurons *in vivo*: role of microglial NADPH oxidase. *J. Neurosci.* **25,** 4082-4090.

Colucci-D'Amato L., Perrone-Capano C. and di Porzio U. (2003) Chronic activation of ERK and neurodegenerative diseases. *Bioessays* **25,** 1085-1095.

Davis R. J. (2000) Signal transduction by the JNK group of MAP kinases. *Cell* **103,** 239-252.

Donovan F. M., Pike C. J., Cotman C. W. and Cunningham D. D (1997) Thrombin induces apoptosis in cultured neurons and astrocytes via a pathway requiring tyrosine kinase and RhoA activities. *J. Neurosci.* **17,** 5316-5326.

Fujimoto S., Katsuki H., Kume T., Kaneko S. and Akaike A. (2004) Mechanisms of oxygen glucose deprivation-induced glutamate release from cerebrocortical slice cultures. *Neurosci. Res.* **50,** 179-187.

Gallo K. A. and Johnson G. L. (2002) Mixed-lineage kinase control of JNK and p38 MAPK

pathways. *Nat. Rev. Mol. Cell. Biol.* **3,** 663-672.

Giovanni A., Sieber B. A., Heikkila R. E. and Sonsalla P. K. (1994) Studies on species sensitivity to the dopaminergic neurotoxin 1-methyl-4-phenyl-1,2,3,6-tetrahydropyridine. Part 1: Systemic administration. *J. Pharmacol. Exp. Ther.* **270,** 1000-1007.

Hamre K., Tharp R., Poon K., Xiong X. and Smeyne, R.J. (1999) Differential strain susceptibility following 1-methyl-4-phenyl-1,2,3,6-tetrahydropyridine (MPTP) administration acts in an autosomal dominant fashion: quantitative analysis in seven strains of *Mus musculus*. *Brain Res.* **828,** 91-103.

Herrera A. J., Tomas-Camardiel M., Venero J. L., Cano J. and Machado A. (2005) Inflammatory process as a determinant factor for the degeneration of substantia nigra dopaminergic neurons. *J. Neural Transm.* **112,** 111-119.

Hirsh E. C., Hunot S., Damier P. and Faucheux B. (1998) Glial cells and inflammation in Parkinson's disease: A role in neurodegeneration. *Ann. Neurol.* **44,** S115-S120.

Iravani M. M., Kashefi K., Mander P., Rose S. and Jenner P. (2002) Involvement of inducible nitric oxide synthase in inflammation-induced dopaminergic neurodegeneration. *Neuroscience* **110,** 49-58.

Jenner P. (2003) Oxidative stress in Parkinson's disease. *Ann. Neurol.* **53 (suppl. 3)**, S26-S38.

Knott C., Stern G. and Wilkin G. P. (2000) Inflammatory regulators in Parkinson's disease: iNOS, lipocortin-1, and cyclooxygenases-1 and -2. *Mol. Cell Neurosci.* **16,** 724-739.

Kreutzberg G. W. (1996) Microglia: a sensor for pathological events in the CNS. *Trends Neurosci.* **19,** 312-318.

Kurkowska-Jastrzebska I., Wronska A., Kohutnicka M., Czlonkowski A. and Czlonkowska A.

(1999) The inflammatory reaction following 1-methyl-4-phenyl-1,2,3,6-tetrahydropyridine intoxication in mouse. *Exp. Neurol.* **156,** 50-61.

Lee D. Y., Oh Y. J. and Jin B. K. (2005) Thrombin-activated microglia contribute to death of dopaminergic neurons in rat mesencephalic cultures: Dual roles of mitogen-activated protein kinase signaling pathways. *Glia* **51,** 98-110.

Liberatore G. T., Jackson-Lewis V., Vukosavic S., Mandir A. S., Vila M., McAuliffe W. G., Dawson V. L., Dawson T. M. and Przedborski S. (1999) Inducible nitric oxide synthase stimulates dopaminergic neurodegeneration in the MPTP model of Parkinson disease, *Nat. Med.* **5,** 1403-1409.

Lipton S. A., Choi Y. B., Pan Z. H., Lei S. Z., Chen H. S., Sucher N. J., Loscalzo J., Singel D. J. and Stamler J. S. (1993) A redox-based mechanism for the neuroprotective and neurodestructive effects of nitric oxide and related nitroso-compounds. *Nature* **364,** 626-632.

Marin-Teva J. L., Dusart I., Colin C., Gervais A., van Rooijen N. and Mallat M. (2004) Microglia promote the death of developing Purkinje cells. *Neuron* **41,** 535-547.

McGeer P. L., Itagaki S., Boyes B. E. and McGeer E. G. (1988) Reactive microglia are positive for HLA-DR in the substantia nigra of Parkinson's and Alzheimer's disease brains. *Neurology* **38,** 1285-1291.

McGeer P. L., Schwab C., Parent A. and Doudet D. (2003) Presence of reactive microglia in monkey substantia nigra years after 1-methyl-4-phenyl-1,2,3,6-tetrahydropyridine adminstration. *Ann. Neurol.* **54,** 599-604.

Noobakhsh F., Vergnolle N., Hollenberg M. D. and Power C. (2003) Proteinase-activated receptors in the nervous system. *Nat Rev. Neurosci.* **4,** 981-990.

Ryu J., Pyo H., Jou I. and Joe E. (2000) Thrombin induces NO release from cultured rat microglia via protein kinase C, mitogen-activated protein kinase and NF-κB. *J. Biol. Chem.* **275,** 29955-29959.

Shibata H., Katsuki H., Nishiwaki M., Kume T., Kaneko S. and Akaike A. (2003) Lipopolysaccharide-induced dopaminergic cell death in rat midbrain slice cultures: role of inducible nitric oxide synthase and protection by indomethacin. *J. Neurochem.* **86,** 1201-1212.

Stoll G. and Jander S. (1999) The role of microglia and macrophages in the pathophysiology of the CNS. *Prog. Neurobiol.* 58, 233-247.

Suo Z., Wu M., Ameenuddin S., Anderson H. E., Zoloty J. E., Citron B. A., Andrade-Gordon P. and Festoff B. W. (2002) Participation of protease-activated receptor-1 in thrombin-induced microglial activation. *J. Neurochem.* **80,** 655-666.

Suo Z., Wu M., Citron B. A., Palazzo R. E. and Festoff B. W. (2003) Rapid tau aggregation and delayed hippocampal neuronal death induced by persistent thrombin signaling. *J. Biol. Chem.* **278,** 37681-37689.

Van Rooijen N. and Sanders A. (1994) Liposome mediated depletion of macrophages: mechanism of action, preparation of liposome and applications. *J. Immunol. Methods* **174,** 83-93.

Xi G., Reiser G. and Keep R. F. (2003) The role of thrombin and thrombin receptors in ischemic, hemorrhagic and traumatic brain injury: deleterious or protective? *J. Neurochem.* **84,** 3-9.

Figure Legends

Fig. 1 Thrombin induces dopaminergic cell death, NO production and whole tissue injury. (a and b) Representative photomicrographs showing TH immunohistochemistry of a slice cultured under control conditions (a) and a slice treated with 300 U/ml thrombin for 72 h (b). Scale bar, 100 μm. (c-g) Concentration-dependent effect of thrombin on the absolute number of dopaminergic neurons (c), nitrite concentrations in culture medium (d), amount of LDH released into culture medium (e), PI uptake into slices (f) and the absolute number of GABAergic neurons (g). Midbrain slice cultures were treated with thrombin at indicated concentrations for 72 h. Number of slices examined for each condition is 10 - 34. Values of nitrite and LDH are of five wells from five independent experiments. * $p < 0.05$, *** $p < 0.001$ vs. control (Cont.).

Fig. 2 Time dependency of thrombin neurotoxicity. Midbrain slice cultures were treated with 300 U/ml thrombin for indicated periods. The absolute number of dopaminergic neurons (a), the amount of nitrite and LDH in medium (b and c, respectively), and the absolute number of GABAergic neurons (d) were quantified. Number of slices examined for each condition is 10 - 29. Values of nitrite and LDH are of five wells from five independent experiments. * $p < 0.05$, ** $p < 0.01$, *** $p < 0.001$ vs. control (Cont.).

Fig. 3 iNOS-derived NO mediates thrombin cytotoxicity on dopaminergic neurons but not on other midbrain cells. (a) Double immunofluorescence shows that intense iNOS immunoreactivities (left) are present in a subpopulation of OX42-positive microglia (right) in midbrain slice cultures treated for 72 h with 300 U/ml thrombin. Arrowheads indicate

examples of doubly positive cells. Scale bar, 50 μm. (b-e) Effect of aminoguanidine on thrombin-induced dopaminergic cell death (b), nitrite increase (c), LDH release (d) and PI uptake (e). Aminoguanidine at indicated concentrations was applied concomitantly with 300 U/ml thrombin for 72 h. Number of slices examined for each condition is 10 - 33. The numbers of culture wells from which values of nitrite and LDH were obtained are indicated in parentheses. *** $p < 0.001$ vs. control (Cont.); # $p < 0.05$, ## $p < 0.01$, ### $p < 0.001$ vs. thrombin alone.

Fig. 4 MAPKs are involved in thrombin-induced cell death and NO production. Effects of PD98059 (a-c), SB203580 (d-f) and SP600125 (g-i) on thrombin-induced dopaminergic cell death (a, d, g), nitrite increase (b, e, h) and LDH release (c, f, i) are shown. PD98059, SB203580 and SP600125 at indicated concentrations were applied concomitantly with 300 U/ml thrombin for 72 h. Number of slices examined for each condition is 9 - 46. The numbers of culture wells examined for nitrite and LDH are indicated in parentheses. ** $p < 0.01$, *** $p < 0.001$ vs. control (Cont.); # $p < 0.05$, ## $p < 0.01$, ### $p < 0.001$ vs. thrombin alone.

Fig. 5 MAPKs are involved in thrombin-induced iNOS expression. (a) Thrombin-induced changes in levels of iNOS, phospho-JNK (p-JNK), phospho-ERK (p-ERK) and phospho-p38 (p-p38). Slice cultures were treated with 300 U/ml thrombin for indicated periods, and lysates were processed for western blot analysis. Blots of iNOS, p-JNK and p-ERK are shown with that of actin, a corresponding loading control. The blot of p-p38 is paired with that of total p38. (b, c) Double immunofluorescence shows that phospho-ERK (b, left) and

phospho-JNK (c, left) are present in OX42-positive microglia (right panels) in midbrain slice cultures treated for 1 h with 300 U/ml thrombin. Scale bars, 50 μm. (d) Time course of phosphorylation of MAPKs in response to 300 U/ml thrombin as revealed by western blot analysis. Levels of phosphorylated MAPKs (p-MAPKs) were normalized by those of actin. n = 5 for p-ERK, n = 4 for p-JNK and n = 3 for p-p38. (e) Time course of iNOS expression in response to 300 U/ml thrombin as revealed by western blot analysis. n = 4 for each time point. ** $p < 0.01$ vs. time 0. (f) Effects of inhibition of MAPKs on thrombin-induced iNOS expression. PD98059 (PD; 100 μM), SB203580 (SB; 30 μM) or SP600125 (SP; 30 μM) was applied concomitantly with 300 U/ml thrombin for 72 h, and expression levels of iNOS protein were examined. Expression levels were normalized by those of glyceraldehyde phosphate dehydrogenase (GAPDH). A representative blot is shown above the graph. n = 5. *** $p < 0.001$ vs. control (Cont.); ### $p < 0.001$ vs. thrombin alone.

Fig. 6 Depletion of microglia protects dopaminergic neurons from thrombin cytotoxicity. (a-d) OX42 immunohistochemistry reveals microglial population within midbrain slice cultures. Compared to control cultures (a), cultures treated with 300 U/ml thrombin for 72 h are characterized by the presence of numerous microglia showing activated morphology (b). Pretreatment of slice cultures with clodronate-containing liposomes (lip.) at indicated doses for 24 h markedly suppressed occupancy of tissues by microglia after thrombin treatment (c, d). Scale bar, 100 μm. (e-g) Effect of clodronate-containing liposomes on thrombin-induced dopaminergic cell death (e), nitrite increase (f) and LDH release (g). Clodronate-containing liposomes were applied at indicated doses to slice cultures for 24 h, which was followed by treatment with 300 U/ml thrombin for 72 h. Number of slices

examined for each condition is 15 - 17. The numbers of culture wells examined for nitrite and LDH are indicated in parentheses. * $p < 0.05$, *** $p < 0.001$ vs. control (Cont.); ## $p < 0.01$, ### $p < 0.001$ vs. thrombin alone.

Fig. 7 Antioxidative drugs protect dopaminergic neurons but not other cells from thrombin cytotoxicity. Effects of FeTPPS (a, b) and *N*-acetylcysteine (c-f) on thrombin-induced dopaminergic cell death (a, c), nitrite increase (d), LDH release (e) and PI uptake (b, f) are shown. FeTPPS and *N*-acetylcysteine were applied at indicated concentrations concurrently with 300 U/ml thrombin for 72 h. Number of slices examined for each condition is 11 - 33 for FeTPPS and 9 - 20 for *N*-acetylcysteine, respectively. The numbers of culture wells examined for nitrite and LDH are indicated in parentheses. *** $p < 0.001$ vs. control (Cont.); # $p < 0.05$, ### $p < 0.001$ vs. thrombin alone.

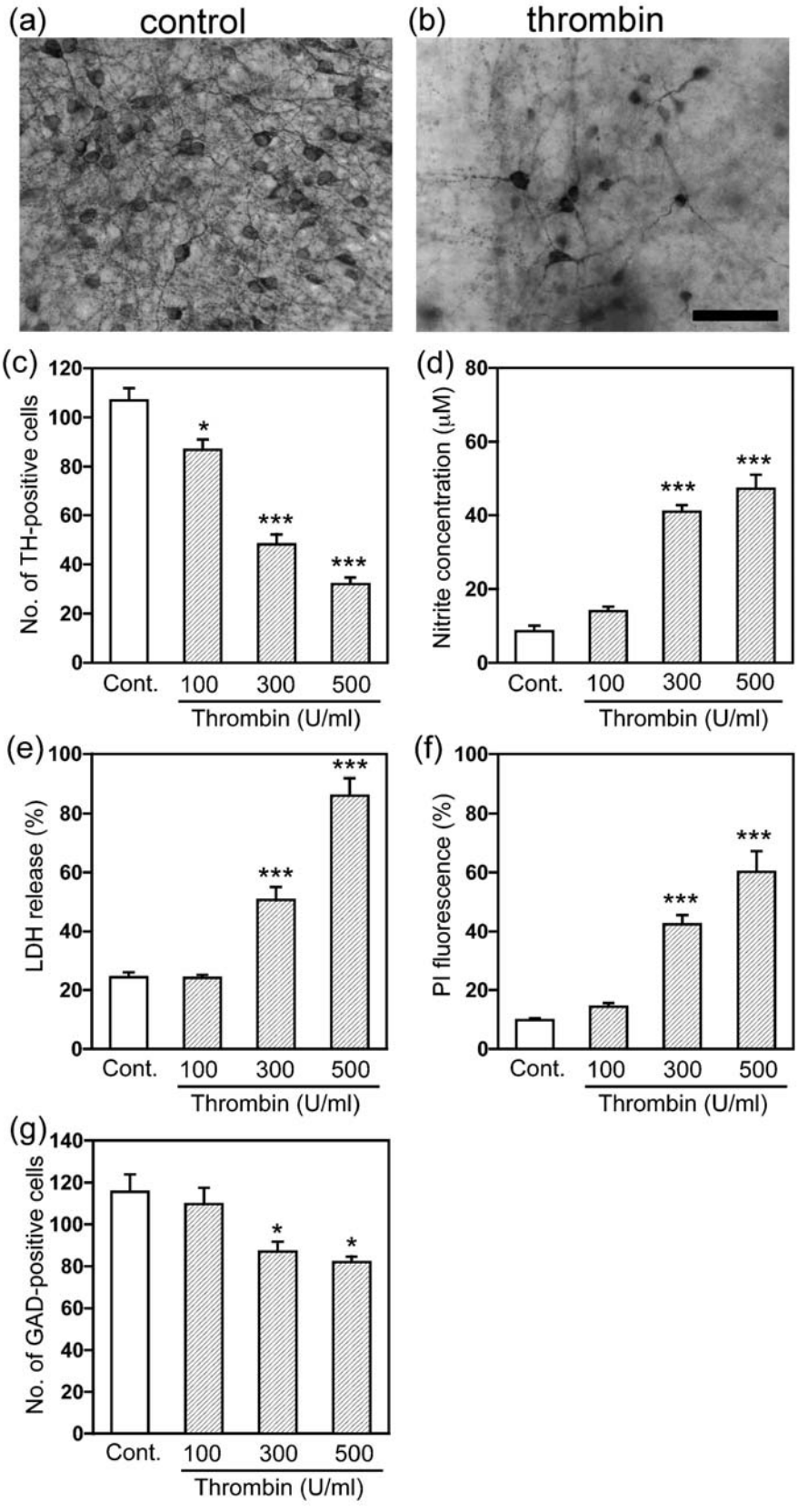
(a) control
(b) thrombin
(c)
No. of TH-positive cells
120
100
80
60
40
20
0
*
***
***
Cont.
100
300
500
Thrombin (U/ml)
(d)
Nitrite concentration (μM)
80
60
40
20
0
***
***
Cont.
100
300
500
Thrombin (U/ml)
(e)
LDH release (%)
100
80
60
40
20
0
***
***
Cont.
100
300
500
Thrombin (U/ml)
(f)
PI fluorescence (%)
100
80
60
40
20
0
***
***
Cont.
100
300
500
Thrombin (U/ml)
(g)
No. of GAD-positive cells
140
120
100
80
60
40
20
0
*
*
Cont.
100
300
500
Thrombin (U/ml)

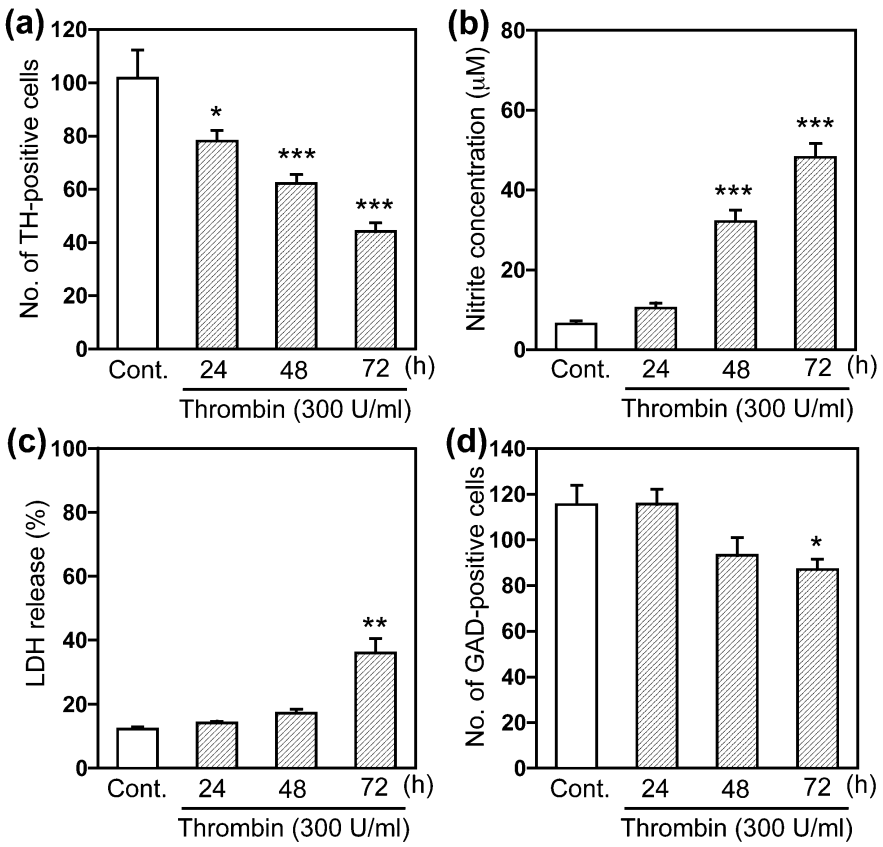
(a)
No. of TH-positive cells
120
100
80
60
40
20
0
*
***
***
Cont.
24
48
72
(h)
Thrombin (300 U/ml)
(b)
Nitrite concentration (μM)
80
60
40
20
0
***
***
Cont.
24
48
72
(h)
Thrombin (300 U/ml)
(c)
LDH release (%)
100
80
60
40
20
0
**
Cont.
24
48
72
(h)
Thrombin (300 U/ml)
(d)
No. of GAD-positive cells
140
120
100
80
60
40
20
0
*
Cont.
24
48
72
(h)
Thrombin (300 U/ml)

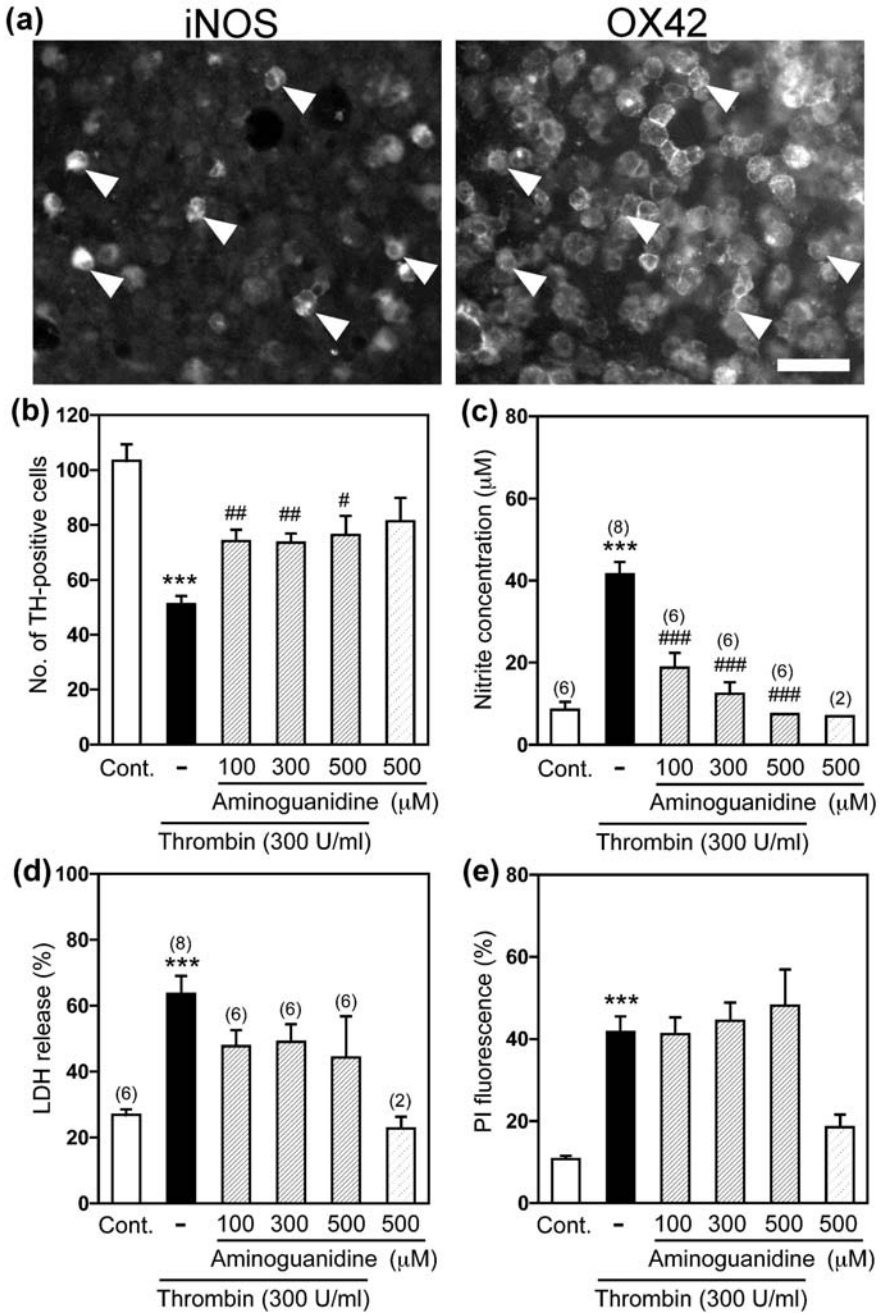
(a)
iNOS
OX42
(b)
No. of TH-positive cells
120
100
80
60
40
20
0
***
##
##
#
Cont.
-
100
300
500
500
Aminoguanidine (μM)
Thrombin (300 U/ml)
(c)
Nitrite concentration (μM)
80
60
40
20
0
(6)
(8)
***
(6)
###
(6)
###
(6)
###
(2)
Cont.
-
100
300
500
500
Aminoguanidine (μM)
Thrombin (300 U/ml)
(d)
LDH release (%)
100
80
60
40
20
0
(6)
(8)
***
(6)
(6)
(6)
(2)
Cont.
-
100
300
500
500
Aminoguanidine (μM)
Thrombin (300 U/ml)
(e)
PI fluorescence (%)
80
60
40
20
0
***
Cont.
-
100
300
500
500
Aminoguanidine (μM)
Thrombin (300 U/ml)

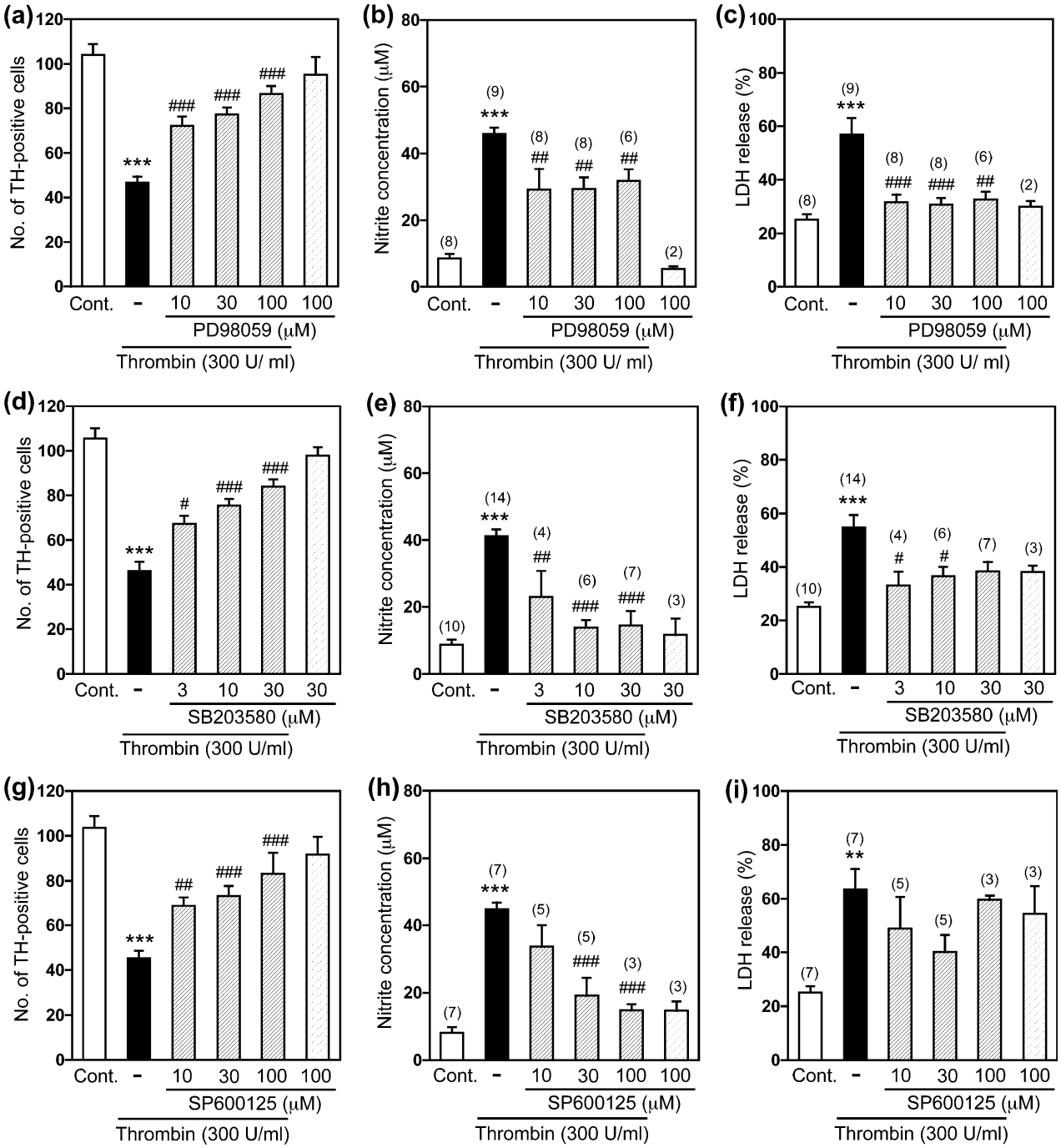
(a)
No. of TH-positive cells
120
100
80
60
40
20
0
***
###
###
###
Cont.
-
10
30
100
100
PD98059 (μM)
Thrombin (300 U/ ml)
(b)
Nitrite concentration (μM)
80
60
40
20
0
(8)
(9)
***
(8)
##
(8)
##
(6)
##
(2)
Cont.
-
10
30
100
100
PD98059 (μM)
Thrombin (300 U/ ml)
(c)
LDH release (%)
100
80
60
40
20
0
(8)
(9)
***
(8)
###
(8)
###
(6)
##
(2)
Cont.
-
10
30
100
100
PD98059 (μM)
Thrombin (300 U/ ml)
(d)
No. of TH-positive cells
120
100
80
60
40
20
0
***
#
###
###
Cont.
-
3
10
30
30
SB203580 (μM)
Thrombin (300 U/ml)
(e)
Nitrite concentration (μM)
80
60
40
20
0
(10)
(14)
***
(4)
##
(6)
###
(7)
###
(3)
Cont.
-
3
10
30
30
SB203580 (μM)
Thrombin (300 U/ml)
(f)
LDH release (%)
100
80
60
40
20
0
(10)
(14)
***
(4)
#
(6)
#
(7)
(3)
Cont.
-
3
10
30
30
SB203580 (μM)
Thrombin (300 U/ml)
(g)
No. of TH-positive cells
120
100
80
60
40
20
0
***
##
###
###
Cont.
-
10
30
100
100
SP600125 (μM)
Thrombin (300 U/ml)
(h)
Nitrite concentration (μM)
80
60
40
20
0
(7)
(7)
***
(5)
(5)
###
(3)
###
(3)
Cont.
-
10
30
100
100
SP600125 (μM)
Thrombin (300 U/ml)
(i)
LDH release (%)
100
80
60
40
20
0
(7)
(7)
**
(5)
(5)
(3)
(3)
Cont.
-
10
30
100
100
SP600125 (μM)
Thrombin (300 U/ml)

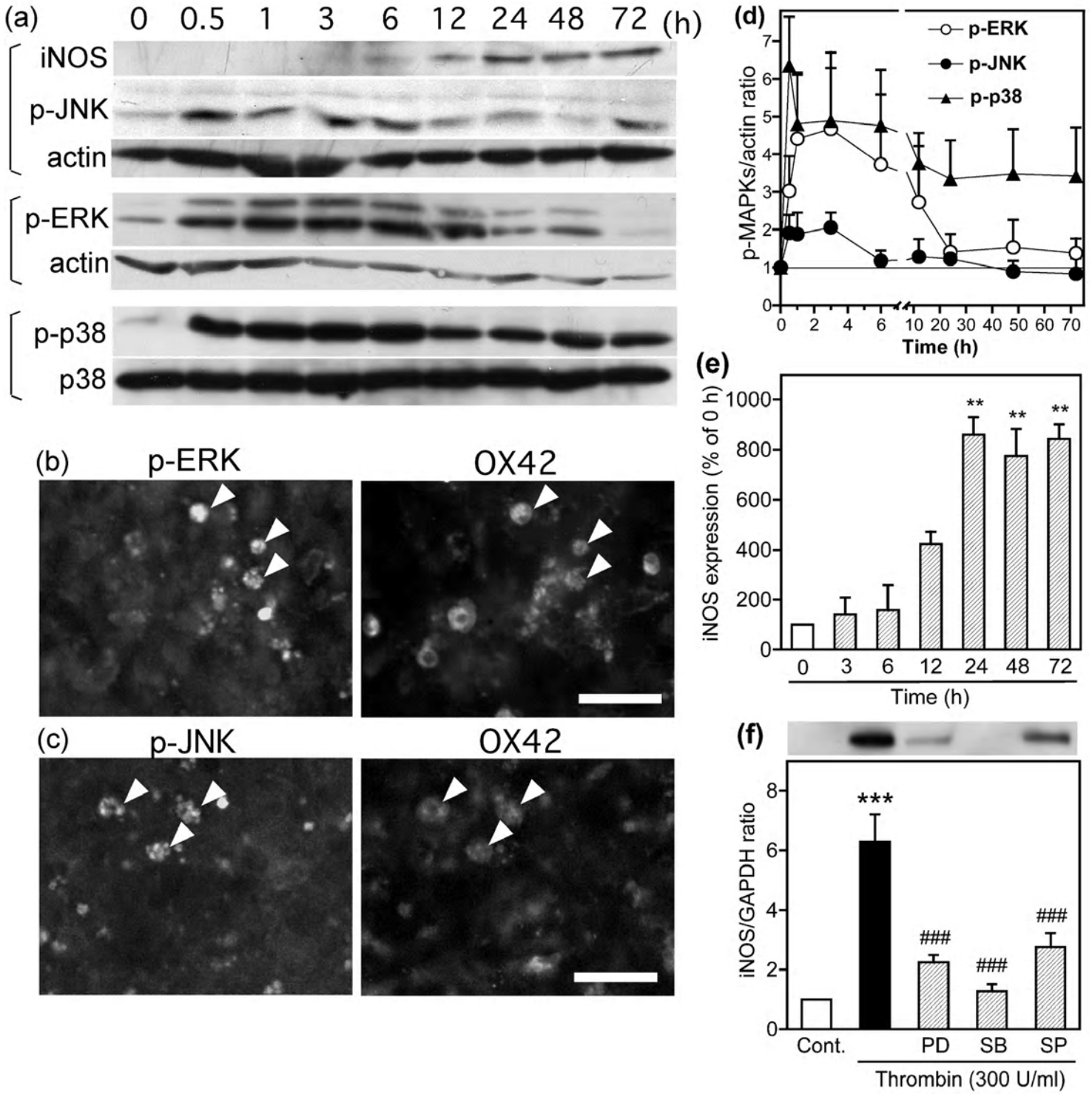
(a)
0 0.5 1 3 6 12 24 48 72 (h)
iNOS
p-JNK
actin
p-ERK
actin
p-p38
p38
(b)
p-ERK
OX42
(c)
p-JNK
OX42
(d)
p-ERK
p-JNK
p-p38
p-MAPKs/actin ratio
Time (h)
(e)
iNOS expression (% of 0 h)
Time (h)
(f)
iNOS/GAPDH ratio
Cont.
PD
SB
SP
Thrombin (300 U/ml)

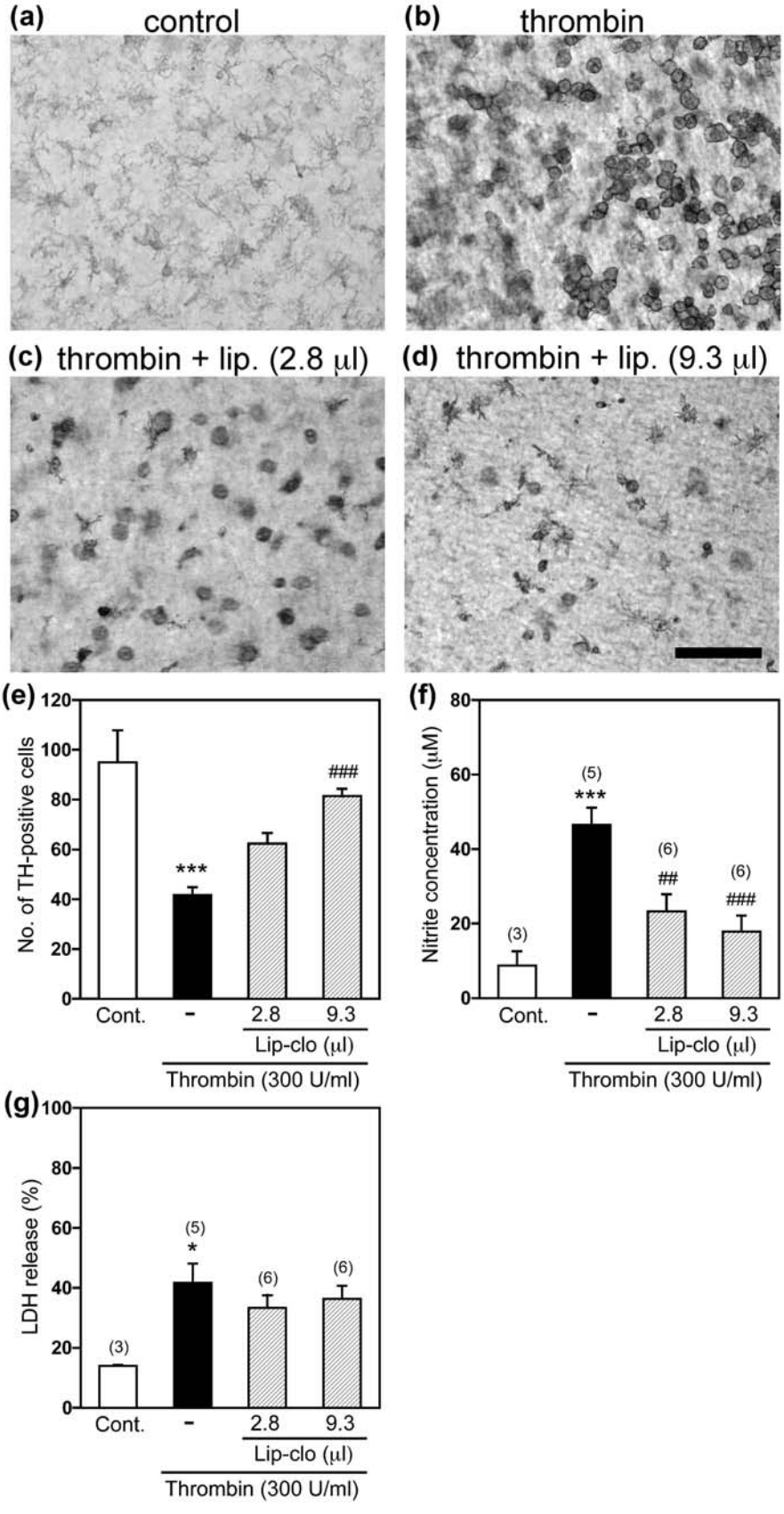
(a) control
(b) thrombin
(c) thrombin + lip. (2.8 μl)
(d) thrombin + lip. (9.3 μl)
(e)
No. of TH-positive cells
120
100
80
60
40
20
0
***
###
Cont.
-
2.8
9.3
Lip-clo (μl)
Thrombin (300 U/ml)
(f)
Nitrite concentration (μM)
80
60
40
20
0
(3)
(5)
***
(6)
##
(6)
###
Cont.
-
2.8
9.3
Lip-clo (μl)
Thrombin (300 U/ml)
(g)
LDH release (%)
100
80
60
40
20
0
(3)
(5)
*
(6)
(6)
Cont.
-
2.8
9.3
Lip-clo (μl)
Thrombin (300 U/ml)

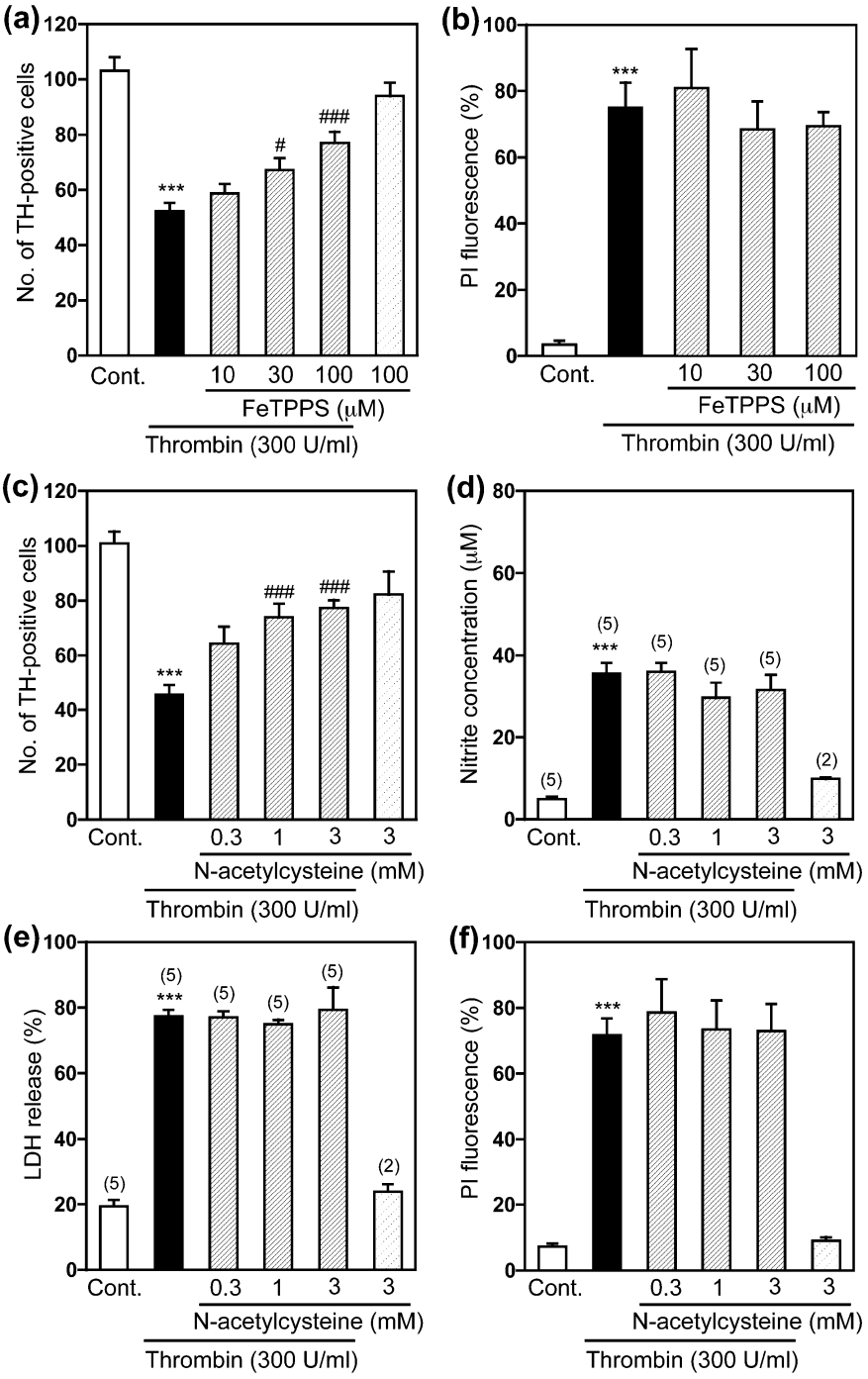
(a)
No. of TH-positive cells
120
100
80
60
40
20
0
***
#
###
Cont.
10
30
100
100
FeTPPS (μM)
Thrombin (300 U/ml)
(b)
PI fluorescence (%)
100
80
60
40
20
0
***
Cont.
10
30
100
FeTPPS (μM)
Thrombin (300 U/ml)
(c)
No. of TH-positive cells
120
100
80
60
40
20
0
***
###
###
Cont.
0.3
1
3
3
N-acetylcysteine (mM)
Thrombin (300 U/ml)
(d)
Nitrite concentration (μM)
80
60
40
20
0
(5)
(5)
***
(5)
(5)
(5)
(2)
Cont.
0.3
1
3
3
N-acetylcysteine (mM)
Thrombin (300 U/ml)
(e)
LDH release (%)
100
80
60
40
20
0
(5)
(5)
***
(5)
(5)
(2)
Cont.
0.3
1
3
3
N-acetylcysteine (mM)
Thrombin (300 U/ml)
(f)
PI fluorescence (%)
100
80
60
40
20
0
***
Cont.
0.3
1
3
3
N-acetylcysteine (mM)
Thrombin (300 U/ml)